Object-Based Classification of Greenhouses Using Sentinel-2 MSI and SPOT-7 Images: A Case Study from Anamur (Mersin), Turkey

Filiz Bektas Balcik, Gizem Senel, and Cigdem Goksel

***Abstract*—Accurate and reliable greenhouse mapping using remotely sensed data and image classification methods has a significant role since it can comprehensively improve the urban and rural planning, and sustainable natural resource and agricultural management. This research is mainly focused on the determination of greenhouses from SPOT-7 and Sentinel-2 MultiSpectral Instrument (MSI) images by using an object-based image classification method with three different classifiers which are k-nearest neighbor (KNN), random forest (RF), and support vector machine (SVM) in the selected test region. First, the image acquired by using multi-resolution segmentation. Second, spectral features, textural features, and remote sensing indices were obtained for each image object. Third, different classifiers were employed to classify greenhouses. Then, classification accuracy assessment analysis was conducted to test the agreement between the classified data and field collected data using the confusion matrix. The results highlighted that the KNN and RF classifier have a slightly higher overall accuracy (OA) and Kappa statistics for SPOT-7 image with the 91.43% and 0.88. Furthermore, the KNN classifier for Sentinel-2 MSI image has the highest OA and Kappa statistics of 88.38% and 0.83. The achieved results underlined the potential of Sentinel-2 MSI and SPOT-7 data for object-based greenhouse mapping using different machine learning classifiers in the Mediterranean Region.**

***Index Terms*—Greenhouse mapping, object-based image analysis (OBIA), random forest (RF), remote sensing, Sentinel-2 MultiSpectral Instrument (MSI), support vector machine (SVM), SPOT-7.**

I. Introduction

THE economic and strategic role of greenhouse activities in agricultural improvement is increasing worldwide, especially as it increases crop yields. However, the extensive and sustained usage of greenhouses results in transformations in the surrounding environment and agricultural areas, together with the essential infrastructure for their commercial operation [1]. Accordingly, proper spatial development planning is inevitable to identify and minimize the effects of these agricultural structures [1]–[3].

Manuscript received February 28, 2020; revised April 13, 2020; accepted May 5, 2020. Date of publication May 28, 2020; date of current version June 19, 2020. *(Corresponding author: Filiz Bektas Balcik.)*

Filiz Bektas Balcik and Cigdem Goksel are with the Civil Engineering Faculty Department of Geomatics Engineering, Istanbul Technical University, İstanbul 34469, Turkey (e-mail: bektasfi@itu.edu.tr; goksel@itu.edu.tr).

Gizem Senel is with the Graduate School of Science, Engineering and Technology, Department of Geomatics Engineering, Istanbul Technical University, İstanbul 34469, Turkey (e-mail: senelgi@itu.edu.tr).

Digital Object Identifier 10.1109/JSTARS.2020.2996315

Remote sensing is a rising data acquisition technique for detecting greenhouses and other land cover types with several spatial and temporal resolutions [4], [5]. However, greenhouse mapping using remotely sensed data is still a challenging and popular research area because of its specific spectral signatures based on its material or local agricultural practices [6].

Greenhouse classification research works have been performed by using numerous pixel-based and object-based classification methods with several remote sensing data, such as Landsat Thematic Mapper [7], Landsat-8 Operational Land Imagery (OLI) [8], the Terra Advanced Spaceborne Thermal Emission and Reflection Radiometer, IKONOS, QuickBird [9], WorldView-2 (WV2) [10], [11], GaoFen-2 [12], and Sentinel-1 and Sentinel-2 MultiSpectral Instruments (MSI) [5].

Aguilar *et al.* [1] mapped greenhouses with an object-based image analysis (OBIA) approach using optical stereo pairs obtained by GeoEye-1 and WV2. They employed both support vector machine (SVM) and nearest neighbor classifiers. The best overall accuracy (OA) result reached 90% by these methods, and obtained results were close to each other. In another investigation, Novelli *et al.* [6] analyzed the efficiency of Sentinel-2 MSI and Landsat-8 OLI to map greenhouses by using OBIA and random forest (RF) classification method. The overall accuracies of the RF classification scheme were achieved higher than 89.0%. Aguilar *et al.* [13] adopted WV2 and Landsat-8 OLI data for mapping greenhouses by using OBIA and decision-tree classification method. Very high OA values were achieved. Hasituya and Chen [4] investigated the usage of multitemporal Landsat-8 OLI imagery to analyze the distribution of greenhouses. Pixel-based RF and SVM methods were used for the analyses. The error matrix results showed a high level of classification accuracy. Lu *et al.* [5] investigated the potential for the combined use of Sentinel-1 synthetic aperture radar and Sentinel-2 MSI data to determine Plastic-Mulched Land-cover (PML). They used and compared three machine-learning classifiers, which are Classification and Regression Tree, RF, and SVM using OBIA. They obtained the best classification result with an OA of 94.34% by using the SVM method. It was also stated that textural information shows a positive effect on PML classification with SVM and RF classifiers. Shi *et al.* [12] proposed a plastic greenhouse mapping method based on the GaoFen-2 image with a three-step procedure. They reached an OA of 97.34%.

There are a limited number of published research studies in the literature about greenhouse detection or determination using remotely sensed data in Turkey. For example, Koc-San [14] aimed to analyze the pixel-based supervised classification methods, which are maximum likelihood (ML), RF, and SVM, to determine greenhouses in Antalya, Turkey. The ability of the WV-2 image for discrimination of plastic and glass greenhouses was also investigated in the research. As a result of the comparison between classification methods, quite high accuracies were obtained. The obtained results showed that all of the used classification methods are considerably successful in the case of plastic greenhouse determination, whereas the SVM and RF classifiers provided significantly higher accuracies than ML for glass greenhouse detection. Balcik *et al.* [15] hypothesized that ground truth data, Sentinel-2 MSI data and several Sentinel-2 MSI image-calculated remote sensing indices using OBIA method will lead to classify greenhouses with sufficient accuracy for the test region in Anamur district of Mersin, located in the Mediterranean region of Turkey. The nearest neighbor object-based classification technique was used with differently created datasets from selected features. The results of the study yield that all created datasets have potential (with an OA over 81%) for greenhouse and surrounding land use and land cover types mapping in the test region.

In this study, the potential of two different satellite images, Sentinel-2 MSI (medium spatial resolution) and SPOT-7 (high spatial resolution) were tested to determine greenhouses using the OBIA method in Anamur district of Mersin, Turkey. The study includes five steps: 1) preprocessing of Sentinel-2 MSI and SPOT-7, 2) segmentation, 3) feature extraction, 4) object-based classification using k-nearest neighbor (KNN), RF, and SVM classifiers, and 5) classification accuracy assessment.

II. Study Area and Data

A. Study Area

In Turkey, the greenhouse activities are managed mainly in the Mediterranean region because of climatic conditions, suitable topography, and sufficient water storage. In this study, a test site from the Mediterranean part of Turkey was selected to determine the ability of Sentinel-2 MSI and SPOT-7 data with OBIA for greenhouse mapping. The selected test area, Anamur District from Mersin, has a huge capacity for agricultural greenhouse activities (see Fig. 1). The area has a typical Mediterranean climate with warm, humid summers; and mild, wet winters. The Anamur district of Mersin is located between the coast and the mountains with a very high level of oxygen and humidity. The region has a capacity of 40% of Turkey's strawberry and banana production with around 3000 greenhouses. Thus, the economy of the region is mainly based on continuous greenhouse agricultural activities.

The Anamur district has a population of 65 920, based on the 2018 Turkey Statistical Institute data. Crop types such as bananas and strawberries are grown in the district, which is located at the western border of Mersin and constitutes 11% of agricultural areas. This region is significant and strategic for greenhouse activities since as nearly all economic and social activities take place in coastal regions.

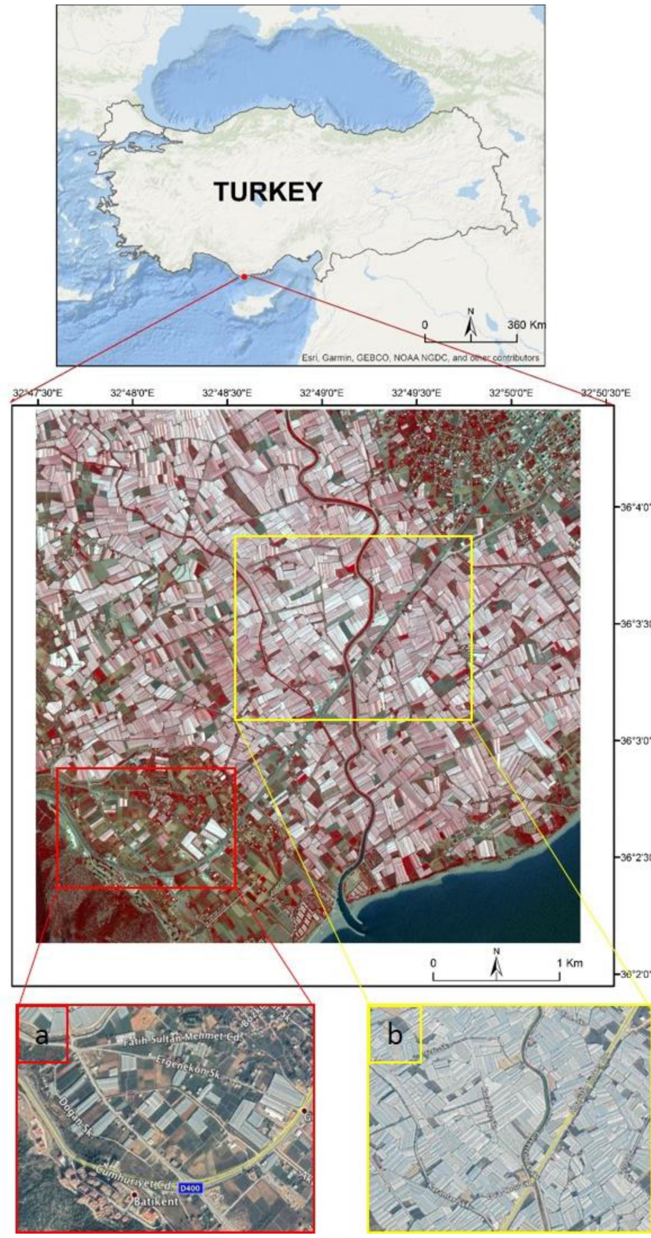

Fig. 1. False-color composite of SPOT-7 image of study area, and distribution of greenhouses in Anamur district from Google Earth: a) dispersed distribution and b) dense distribution.

B. Data

High-resolution SPOT-7 scene from August 2, 2018 and new-generation freely available medium spatial resolution Sentinel-2 MSI scene from August 2, 2018 were used in the research. The specifications of used data were given in Table I.

Sentinel-2 MSI is a multispectral imaging instrument that was launched in June 2015. Sentinel-2 MSI provides multispectral images with various spatial and spectral resolutions with a swath width of 290 km. It acquires images with 13 bands with different spatial resolutions ranging between 10 and 60 m. Visible and

TABLE I
USED BAND SPECIFICATIONS

Sensor	Bands	Wavelength range (μm)	Resolution (m)
Spot-7	Band 1 - Blue	0.455-0.525	6
	Band 2 - Green	0.530-0.590	6
	Band 3 - Red	0.625-0.695	6
	Band 4 - NIR	0.760-0.890	6
	Band 5 - Panchromatic	0.450-0.745	1.5
Sentinel-2 MSI	Band 2 - Blue	0.439-0.535	10
	Band 3 - Green	0.537-0.582	10
	Band 4 - Red	0.646-0.685	10
	Band 8 - NIR	0.767-0.908	10

near-infrared (NIR) bands have 10-m spatial resolution. On the other hand, red-edge and shortwave infrared bands have 20-m spatial resolution [16]. In this study, four bands of Sentinel-2 MSI with 10 m spatial resolutions were used.

SPOT-7 satellite sensor launched in 2014 built by AIRBUS Defence & Space. It has red, green, blue, and NIR bands with 6-m spatial resolution and a panchromatic band with 1.5-m spatial resolution. The radiometric resolution of the SPOT-7 image is 12 bit. Four bands of Sentinel-2 MSI, which has a 10-m resolution, and four bands of SPOT-7 image were used for the OBIA.

III. Methodology

The aim of the study is to delineate the distribution of greenhouses in the region using satellite images and OBIA method. This method was applied to determine greenhouses by using SPOT-7 and Sentinel-2 MSI data and variate classification methods such as RF, SVM, and KNN. A flowchart of the study is given in Fig. 2 and conducted research steps were explained in the following sections.

A. Image Preprocessing Stage

The Sentinel-2 MSI image was atmospherically corrected using Sen2Cor Processor [17] in SNAP software to obtain the Level 2A image. Then, to enhance the spatial resolution of the SPOT-7 image, one of the most widespread and best-performing fusion methods, Gram–Schmidt spectral sharpening method was applied, which was proposed by Laben and Brover in 1998 and patented by Eastman Kodak [18]. This method is based on the decorrelation of the input bands using their covariance values. The main reason for using this method is that it has noticeable advantages in improving spatial information while preserving its spectral information. Besides, the geometric correction was applied by using ground control points to coregister Sentinel-2 MSI and SPOT-7 pan-sharpen data with root mean square error less than 0.5 pixels.

B. Segmentation

Image segmentation is the first stage of the OBIA, where the image is segmented into homogeneous and discrete objects based on color, spectral characteristics, similar texture, and shape of objects. Multiresolution segmentation (MRS) is a bottom-up region merging procedure [19], [20], which is

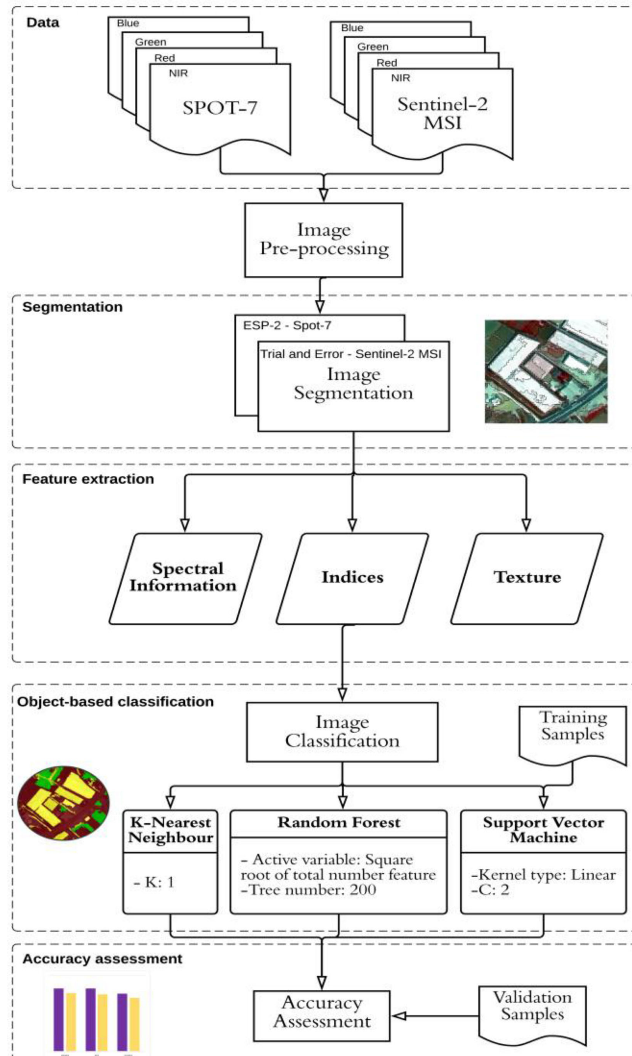

Fig. 2. Flowchart of the research.

proved to be the most notable segmentation method with several iterative steps to create large objects from smaller ones, was chosen to segment the Sentinel-2 MSI satellite image. The significant part of the object-based classification is the selection of the best parameter combination, specifically optimal scale parameter (SP) in MRS [5].

The result of the MRS method is regulated by three parameters, which are shape, SP, and compactness. SP can be explained by the maximum heterogeneity for the created segment. Likewise, compactness is defined as the weight of the smoothness criteria whereas the shape parameter determines the weight of color and shape criteria [21].

To select SP objectively, first, estimation of SP-2 (ESP-2) tool introduced by Drăguţ *et al.* [22], [23], [24] was employed in this study. However, although this method showed appropriate results for the SPOT-7 image, it created objects larger than the desired object size for the Sentinel-2 MSI image. For this reason, ESP-2 tool was preferred for SPOT-7, whereas trial and error approach was used for Sentinel-2 MSI.

Three components were determined with a systematic trial-and-error method via visual interpretation of data. Object-based image processing procedures were performed using eCognition Developer 9.0 software [25].

Similar to conducted studies [22], [26], the compactness parameter was established to 0.5, which balances compactness and smoothness. The five separate values {0.1, 0.3, 0.5, 0.7, 0.9} of shape parameter was specified and different values for SP were analyzed in MRS. The effects of these values on the segmentation have been assessed by the visual analysis, which is widely used in the selection of segmentation parameters [27].

ESP-2 tool, which is programmed in eCognition Network Language within eCognition was used to segment the SPOT-7 image. ESP-2 tool is an automated procedure parameterizing multiscale image segmentation of multiple layers accessible through eCognition software. This tool takes advantage of local variance (LV) for determining scale transition by detecting the layer numbers and segments them iteratively with the MRS algorithm. The optimal SP is selected automatically where LV at level n (LV_n) is equal or lower than the LV at level n–1 (LV_{n-1}) [22].

Two values {0.1 and 0.3} of shape parameters were tested in this work by setting compactness to 0.5 as in the trial and error approach. These two combinations were tested in both nonhierarchy and hierarchy options. For each one of these four combinations of parameters and options, the ESP-2 tool was analyzed through eCognition. Since produced second- and third-level segments were much bigger than a single greenhouse, these levels were not taken into consideration.

C. Feature Selection and Extraction

The image segmentation makes it possible for the extraction of features linked with image objects. Owing to the growing seasons of the crops, the topography, and the geography of the region, it is inevitable to combine spectral and spatial information to obtain accurate mapping, as the spectral characteristics of greenhouses have changed. Fig. 3 showed the reflectance curve of the main land use and land cover categories for the SPOT-7 and Sentinel-2 MSI. Reflectance curves that belong to greenhouses were differentiated from the other categories for the blue, green, and red regions of SPOT-7 and Sentinel-2 MSI. In the NIR region, greenhouses and vegetation categories have very similar reflectance values.

The object-based features used in this study are shown in Table II. The selection of the features was mainly based on literature review [13]. 1) Mean, standard deviation of four bands, brightness, and differences were included as spectral information of each created object. 2) Widely used remote sensing indices, which are normalized difference vegetation index (NDVI) and normalized difference water index (NDWI) were employed. 3) Finally, textural information was also included in research since it is a significant consideration in object-based classification. Textural features indicate local spatial information that is relevant to tonal variations in the remotely sensed data. Textural information was derived from the gray level co-occurrence Matrix (GLCM) proposed by Haralick *et al.* [28].

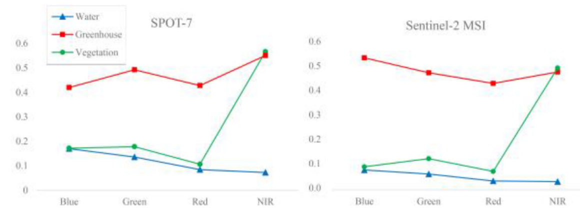

Fig. 3. Spectral signatures of greenhouse, vegetation, and water classes belonging to different transects.

TABLE II
EXTRACTED FEATURES

Category	Feature	Description	Reference
Spectral Information	Mean	Mean values of four bands for each image objects	[25]
	Standard Deviation	Standard deviation of four bands for each image objects	[25]
	Brightness	Brightness of the optical image layers	[25]
	Difference	Max difference of brightness	[25]
Indices	NDVI	(NIR-Red)/(NIR+Red)	[29]
	NDWI	(Green- NIR)/(Green+ NIR)	[30]
Textural Information	GLCM ASM	Angular 2nd moment of all directions	[28]
	GLCM CON	Contrast of all directions	[28]
	GLCM COR	Correlation of all directions	[28]
	GLCM DIS	Dissimilarity of all directions	[28]
	GLCM ENT	Entropy of all directions	[28]
	GLCM HOM	Homogeneity of all directions	[28]

Textural features computed using GLCM, including angular second moment (ASM), contrast (CON), correlation (COR), dissimilarity (DIS), entropy (ENT), and homogeneity (HOM), all of which are widely used for object-based classification. These above-mentioned features were used as input variables to train classifiers (KNN, RF, and SVM).

D. Classification Methods

The mapping performance of the three classification methods (KNN, RF, and SVM) were tested in this research due to challenging spectral characteristics of greenhouses.

KNN, which is an instance-based learning method [31], [32], is commonly characterized as one of the simplest machine learning classifiers. This method image objects depend on the nearest training samples in the feature space. Neighborhood value k is an essential component of KNN method, which significantly affects the classification result. The distance between each unknown object and its closest neighbors can be measured, so if most neighboring occurrences of the unknown object belong to a class, that object can be located in the same category. K parameter was chosen based on the literature search as 1 in this study.

TABLE III
VALIDATION AND TRAINING SAMPLES

			Greenhouse	Other	Vegetation	Water
Spot-7	T.S.	N.O.	185	190	53	114
		N.P.	225703	368368	106426	197882
Sentinel-2 MSI	T.S.	N.O.	145	191	51	18
		N.P.	6160	10118	2124	5414
Validation Sample			131	205	115	74

N.O. Number of object; N.P. Number of pixel; T.S.Training sample

The other classification method used for mapping greenhouses is RF classifier. RF is a machine learning technique, which trained each tree by sampling the training dataset and a set of variables separately through bagging or bootstrap aggregating [33]. The number of active variables in the random subset at each node and the number of trees in the forest are two parameters of RF. The number of active variables was set to the square root of the features numbers whereas the number of trees was fixed to 200.

The last method used in the research is SVM, which is introduced by Cortes and Vapnik [34]. It is an advanced non-parametric machine learning algorithm. This method is designed for finding an optimal decision hyperplane in high-dimensional space to produce optimal discrimination of classes. For the SVM classifier, the linear function was selected and the cost of constraints (C) was chosen as 10^2.

E. Accuracy Assessment

This study evaluated the accuracy for each of the classification results by using the error matrix calculated with validation samples. User's accuracy (UA), and producer's accuracy (PA) for each class, OA, and the Kappa coefficient [35] are calculated to assess the performance of the classification. The ground truth including field survey, geo-tagged field photos, and collected GPS data for the project entitled as "Mersin Environmental Plan and Research and Analytical Survey for the Whole City" and high-resolution Google Earth images were used to prepare training and validation dataset. Validation points were used to determine the accuracy of classification results (see Table III).

IV. RESULTS

A. Segmentation Results

To find the ideal SP for best segmentation result of Spot-7 and Sentinel-2 MSI images, ESP-2, and trial-and-error approach were used, respectively.

We found that SP 39 is appropriate for detecting greenhouses from Sentinel-2 MSI after testing different SP values while keeping the compactness parameter at 0.5 and shape at 0.3.

ESP-2 tool were employed to calculate SP for SPOT-7. As a result of the four combinations mentioned in the methodology section, the SP calculated from ESP-2 tool had values ranging from 140 to 199. Here, the SP was chosen as 140 since it was seen that some objects contain greenhouses merging with the roads around it in the other combinations. The SP 140 was calculated using the nonhierarchy option, fixing the shape value to 0.1 and the compactness value to 0.5. However, it must be noted that the nonhierarchy option took a longer time (approximately 4 h) than the hierarchy option (approximately 20 min) in our case. The best segmentation results for both SPOT-7 and Sentinel-2 MSI in a sample region are given in Fig. 4.

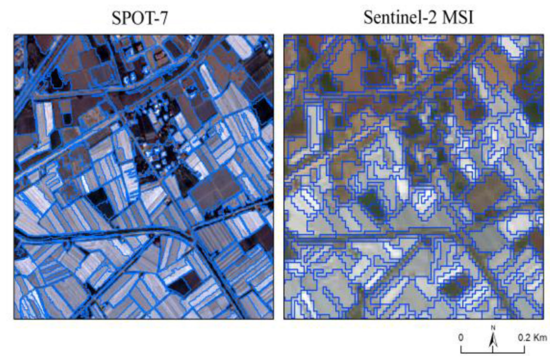

Fig. 4. Segmentation results for SPOT-7 and Sentinel-2 images in a sample region.

TABLE IV
OA AND KAPPA RESULTS

	Overall Accuracy		Kappa	
	SPOT-7	Sentinel-2 MSI	SPOT-7	Sentinel-2 MSI
KNN	91.43%	88.38 %	0.88	0.83
RF	91.43%	87.62%	0.88	0.82
SVM	88.00%	85.14%	0.83	0.78

B. Classification Results

Within the scope of this study, SPOT-7 and Sentinel-2 MSI images were classified using object-based KNN, RF, and SVM methods to determine the greenhouses and surrounding land cover and land use types. Greenhouse, vegetation, water surface, and others that include bare land, artificial surface, built-up, and road classes were determined as land cover and land use categories. For the classification procedure, 442 training objects for SPOT-7 and 405 training objects for Sentinel-2 MSI were collected and 525 randomly selected validation points were generated. The detailed information about training and validation samples were given in Table III. According to the selected training samples, classification was applied based on object-based KNN, RF, and SVM methods by using the remote sensing indices, spectral information, and textural features. The classified maps produced from SPOT-7 and Sentinel-2 MSI are given in Fig. 5.

Accuracy assessment was carried out based on the error matrix. Table IV and Fig. 6 summarize the classification accuracy assessment results. Regarding the OA and kappa values obtained from the accuracy assessment of classified SPOT-7 and Sentinel-2 MSI for the entire study area, the results from SPOT-7 KNN and RF (OA = 91.43%; Kappa = 0.88) were slightly better than those attained from Sentinel-2 MSI KNN and RF (OA = 88.38%; Kappa: 0.83 for KNN and OA = 87.62%;

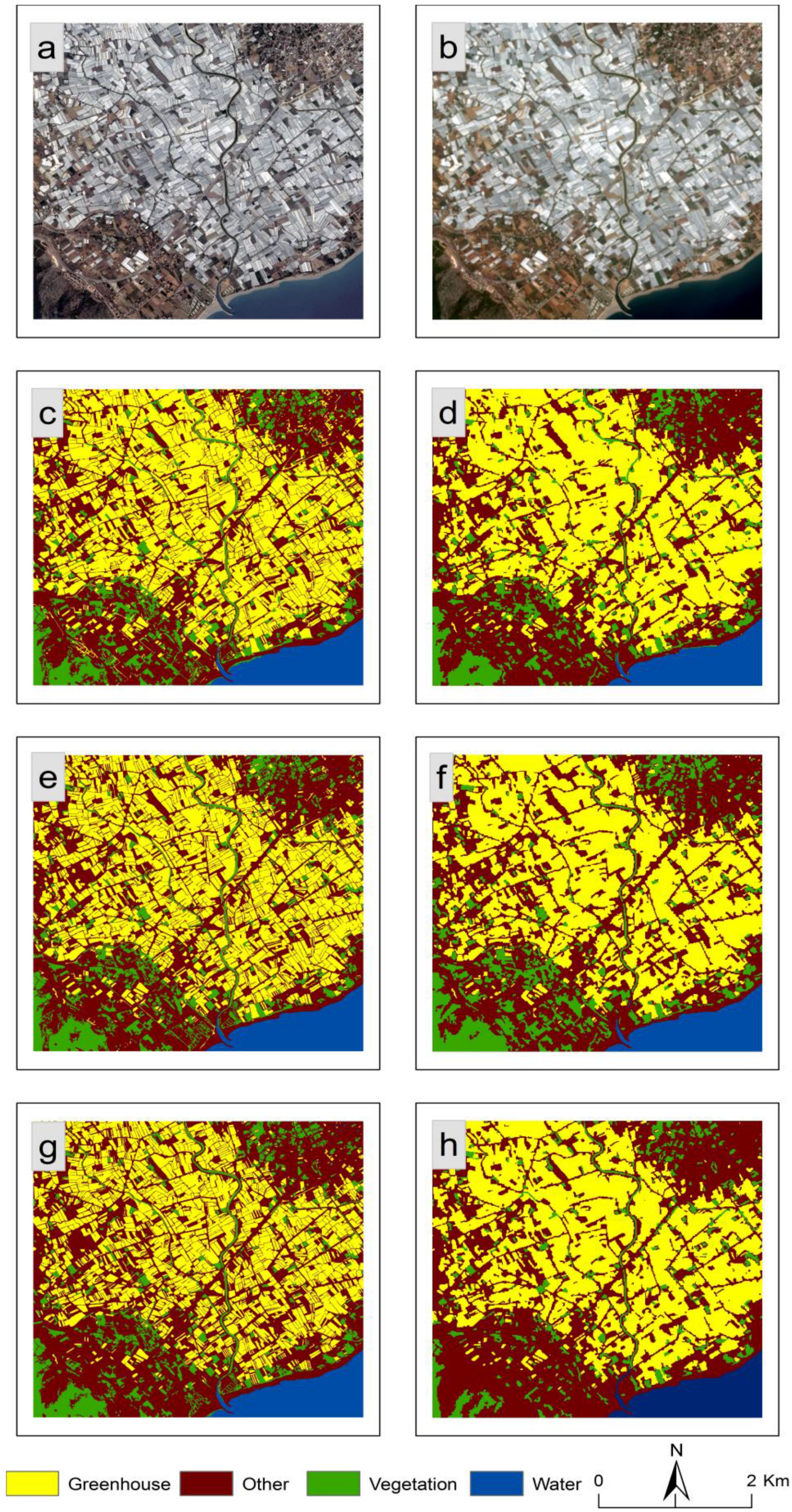

Fig. 5. True-color images of (a) SPOT-7, (b) Sentinel-2 MSI, and classification results of (c) SPOT-7—KNN, (d) Sentinel-2 MSI—KNN, (e) SPOT-7—RF, (f) Sentinel-2 MSI—RF, (g) SPOT-7—SVM, and (h) Sentinel-2 MSI—SVM.

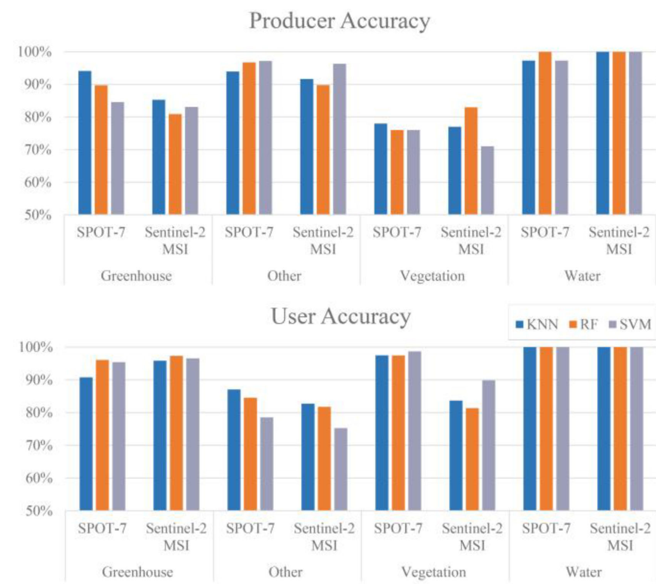

Fig. 6. Producer and user accuracy results for SPOT-7 and Sentinel-2 MSI for each land cover categories.

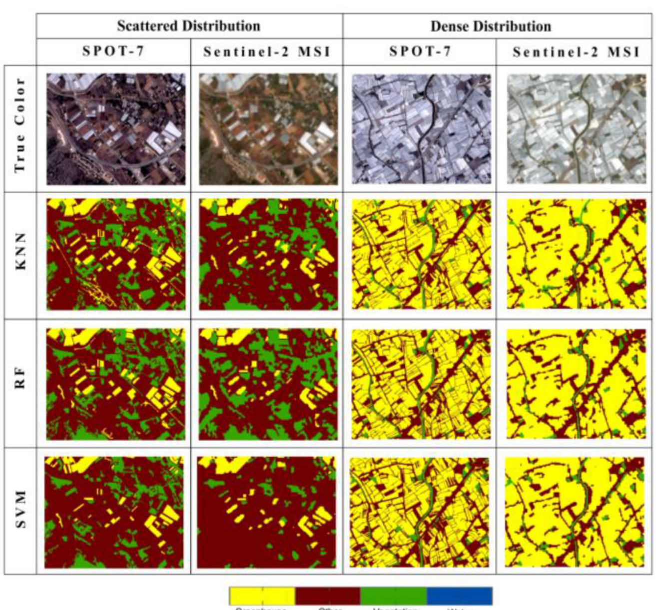

Fig. 7. Classification results of the classifiers in scattered and dense distribution of greenhouses (test regions in Fig. 1).

Kappa: 0.88 for RF). These results show that the SVM classifier underperformed than the KNN and RF classifiers.

Based on calculated UA and PA, it can be said that all classified images show satisfactory performance not only for greenhouse mapping but also for other land cover types. The classification accuracies for greenhouse were greater than 83% in terms of PA and 95% in terms of UA.

The PA for the greenhouse class was always better than the PA of the other class for selected satellite images and three classifiers. These result confirmed the high classification accuracy achieved from the KNN and RF classifiers for the greenhouse class. Especially for two datasets, other class was mixed with vegetation class due to the mountainous area, which covers sparsely vegetated surfaces in the test area. Apart from this, roof structure of rural area settlements was mixed with greenhouses in classification results derived from RF and SVM classifiers for both of the two datasets. Novelli *et al.* [6] explained this situation as a result of the high heterogeneity of the region.

When we compare the potential of two satellite images, the result show that SPOT-7 has slightly better accuracy than Sentinel-2 MSI due to its high spatial resolution.

V. Discussion

With the rapid evolution of new-age agriculture activities, greenhouse mapping research studies have increased lately along with the several classifiers based on remote sensing satellite images such as Sentinel-2 MSI, Landsat-8 OLI, and WV-2. In this study, object-based classification was employed to determine greenhouses that are sparsely and frequently located in a heterogeneous test region. Moreover, the effectiveness of the three machine-learning based classifiers was tested using two satellite images with different spatial resolutions (SPOT-7 with 1.5 m and Sentinel-2 MSI with 10 m).

Object-based classification offers many advantages compared to the traditional pixel-based classification, as stated by Wu *et al.* [36]. OBIA was used in this research since it helps to avoid the salt-and-pepper effect and to utilize textural properties of objects in addition to the traditional spectral characteristics.

As the first step of object-based classification, image segmentation was conducted. Shape and compactness parameters for MRS were determined based on a trial-and-error approach and existing influential studies. ESP-2 tool and trial-and-error approaches were employed to determine SP. ESP-2 tool was not satisfactory for the Sentinel-2 MSI image in our case. However, it was used to determine an ideal SP for the SPOT-7 image. The critical issue that must be considered when using the ESP-2 tool is that the nonhierarchy option takes too much time.

The pixel-based mapping methods by using advanced classification methods are able to get accuracies over 90% [14]. On the contrary, object-based mapping methods with the integration of texture and remote sensing indices were reported to obtain accuracies over 95% [6]. By comparison, in our study, two satellite data with a different spatial resolution were used together with selected features and advanced classification methods. Thereby, competitive accuracy results were achieved, especially for greenhouses. As depicted in Table IV, the classification accuracy of KNN and RF classifiers (OA of 91.43%) is higher than the SVM classifier (OA of 88.00%) for SPOT-7 data. Additionally, the KNN classifier (88.38%) reached higher classification accuracy than RF (OA of 87.62%) and SVM (OA of 85.14%) classifiers for Sentinel-2 MSI data. The classification results obtained with advanced classification algorithms using two different spatial resolutions have similarities in terms of accuracy assessment. However, each classifier has its advantages and disadvantages from the point of greenhouse mapping since training samples and the classifier parameters will affect the accuracy. In this manner, the selection of suitable classifiers may change case by case.

Different natural structures, regular and irregular residential areas and rural areas in the selected region lead to the mixing of greenhouses with the other categories such as artificial surfaces. As mentioned in the other studies [6], heterogeneity of the region is the main reason of this misclassification of greenhouses. Considering the visual interpretation of scattered greenhouse distribution in the region, it was observed that the roads and bare lands were incorrectly classified as a greenhouse using KNN and RF methods in the SPOT-7 image (see Fig. 7).

Similarly, in Sentinel-2 MSI images, some bare land surfaces were classified as a greenhouse with KNN and RF methods, whereas some white-roofed buildings were classified as a greenhouse in the SVM method. On the contrary, in regions with densely distributed greenhouses, the misclassification occurred in the SVM method due to the reflection on the greenhouse roof. Despite these mixing problems, the selected data and suggested methodology provided satisfactory results for mapping greenhouses.

VI. Conclusion

Greenhouse cultivation is a practice used to improve and increase food production. Nevertheless, their development has major negative influences on our environment. With the rapid expansion of greenhouse activities, the need to reveal the amount and distribution inventories of greenhouses with advanced technologies has emerged.

In this study, object-based greenhouse mapping based on three machine-learning based classifiers was carried out using SPOT-7 and Sentinel-2 MSI images in Anamur District. This article contributes to the literature since there is a limited number of conducted greenhouse mapping studies in Turkey by using different remotely sensed data. Furthermore, as per our knowledge, this is the first study to investigate the detection of greenhouse areas by classifying Sentinel-2 MSI and SPOT-7 satellite images using object-based methods. The combination of spectral (including remote sensing indices) and textural features provided competitive accuracy for greenhouse mapping while using both SPOT-7 and Sentinel-2 images, especially for KNN and RF methods. Further research will be focused on both the improvement of segmentation process and the determination of new features for greenhouse mapping using Sentinel-2 MSI and SPOT-7 with different scenarios.

Acknowledgment

The authors would like to thank Istanbul Technical University Application and Research Center for Satellite Communications and Remote Sensing for providing the SPOT-7 satellite image. We also would like to thank the "Mersin Metropolitan Municipality" and "Promer Planning Engineering and Trade Inc." for providing the ground truth studies within the scope of the "Mersin Environmental Plan and Research and Analytical Survey for the Whole City" project.

References

[1] M. A. Aguilar, F. Bianconi, F. J. Aguilar, and I. Fernández, "Object-based greenhouse classification from GeoEye-1 and WorldView-2 stereo imagery," *Remote Sens.*, vol. 6, no. 5, pp. 3554–3582, 2014.

[2] F. Agüera, F. J. Aguilar, and M. A. Aguilar, "Using texture analysis to improve per-pixel classification of very high resolution images for mapping plastic greenhouses," *ISPRS J. Photogramm. Remote Sens.*, vol. 63, no. 6, pp. 635–646, 2008.

[3] D. Yang, J. Chen, Y. Zhou, X. Chen, X. Chen, and X. Cao, "Mapping plastic greenhouse with medium spatial resolution satellite data: Development of a new spectral index," *ISPRS J. Photogramm. Remote Sens.*, vol. 128, pp. 47–60, 2017.

[4] Hasituya and Z. Chen, "Mapping plastic-mulched farmland with multi-temporal Landsat-8 data," *Remote Sens.*, vol. 9, no. 6, pp. 1–27, 2017.

[5] L. Lu, Y. Tao, and L. Di, "Object-based plastic-mulched landcover extraction using integrated Sentinel-1 and Sentinel-2 data," *Remote Sens.*, vol. 10, no. 11, pp. 1–18, 2018.

[6] A. Novelli, M. A. Aguilar, A. Nemmaoui, F. J. Aguilar, and E. Tarantino, "Performance evaluation of object based greenhouse detection from Sentinel-2 MSI and Landsat 8 OLI data: A case study from Almería (Spain)," *Int. J. Appl. Earth Observ. Geoinf.*, vol. 52, pp. 403–411, 2016.

[7] P. Picuno, A. Tortora, and R. L. Capobianco, "Analysis of plasticulture landscapes in Southern Italy through remote sensing and solid modelling techniques," *Landsc. Urban Plan.*, vol. 100, nos. 1/2, pp. 45–56, 2011.

[8] A. Novelli and E. Tarantino, "Combining ad hoc spectral indices based on LANDSAT-8 OLI/TIRS sensor data for the detection of plastic cover vineyard," *Remote Sens. Lett.*, vol. 6, no. 12, pp. 933–941, 2015.

[9] C. Arcidiacono and S. M. C. Porto, "Pixel-based classification of high-resolution satellite images for cropshelter coverage recognition," *Acta Horticulturae*, vol. 937, pp. 1003–1010, 2012.

[10] K. Tasdemir and D. Koc-San, "Unsupervised extraction of greenhouses using approximate spectral clustering ensemble," in *Proc. IEEE Int. Geosci. Remote Sens. Symp.*, Quebec City, QC, Canada, Jul. 13–18, 2014, pp. 4914–4917.

[11] E. Tarantino and B. Figorito, "Mapping rural areas with widespread plastic covered vineyards using true color aerial data," *Remote Sens.*, vol. 4, no. 7, pp. 1913–1928, 2012.

[12] L. Shi, X. Huang, T. Zhong, and H. Taubenböck, "Mapping plastic greenhouses using spectral metrics derived from GaoFen-2 satellite data," *IEEE J. Sel. Topics Appl. Earth Observ. Remote Sens.*, vol. 13, pp. 49–59, 2020.

[13] M. A. Aguilar, A. Nemmaoui, A. Novelli, F. J. Aguilar, and A. G. Lorca, "Object-based greenhouse mapping using very high resolution satellite data and Landsat 8 time series," *Remote Sens.*, vol. 8, no. 6, pp. 10–12, 2016.

[14] D. Koc-San, "Evaluation of different classification techniques for the detection of glass and plastic greenhouses from WorldView-2 satellite imagery," *J. Appl. Remote Sens.*, vol. 7, no. 1, 2013, Art. no. 073553.

[15] F. Bektas Balcik, G. Senel, and C. Goksel, "Greenhouse mapping using object based classification and sentinel-2 satellite imagery," in *Proc. 8th Int. Conf. Agro-Geoinformat.*, Istanbul, Turkey, 2019, pp. 1–5.

[16] M. Drusch *et al.*, "Sentinel-2: ESA's optical high-resolution mission for GMES operational services," *Remote Sens. Environ.*, vol. 120, pp. 25–36, 2012.

[17] U. Muller-Wilm, J. Louis, R. Richter, F. Gascon, and M. Niezette, "Sentinel-2 level 2A prototype processor: Architecture, algorithms and first results," in *Proc. ESA Living Planet Symp.,* Edinburgh, U.K., Sep. 9–13, 2013, p. 98.

[18] C. A. Laben, and B. V. Brower, "Process for enhancing the spatial resolution of multispectral imagery using pansharpening," U.S. Patent # 6 011 875, 2005, 2000.

[19] M. Baatz and M. Schäpe, "Multiresolution segmentation—An optimization approach for high quality multi-scale image segmentation," in *Proc. Angewandte Geographische Inf.-Verarbeitung XII*, Karlsruhe, Germany, 2010, pp. 12–23.

[20] D. C. Duro, S. E. Franklin, and M. G. Dubé, "Comparison of pixel-based and object-based image analysis with selected machine learning algorithms for the classification of agricultural landscapes using Spot-5 HRG imagery," *Remote Sens. Environ.*, vol. 118, pp. 259–272, 2012.

[21] J. Tian and D. M. Chen, "Optimization in multi-scale segmentation of high resolution satellite images for artificial feature recognition," *Int. J. Remote Sens.*, vol. 28, pp. 4625–4644, 2007.

[22] L. Drăguţ, O. Csillik, C. Eisank, and D. Tiede, "Automated parameterisation for multi-scale image segmentation on multiple layers," *ISPRS J. Photogramm. Remote Sens.*, vol. 88, pp. 119–127, 2014.

[23] L. Drăguţ, D. Tiede, and S. R. Levick, "ESP: A tool to estimate scale parameter for multiresolution image segmentation of remotely sensed data," *Int. J. Geographical Inf. Sci.*, vol. 24, no. 6, pp. 859–871, 2010.

[24] L. Drăguţ and C. Eisank, "Automated object-based classification of topography from SRTM data," *Geomorphology*, vol. 141–142, pp. 21–33, 2012.

[25] eCognition Developer 9.0.1 Reference Book, Trimble Germany GmbH, Munich, Germany, 2014.

[26] D. Liu and F. Xia, "Assessing object-based classification: Advantages and limitations," *Remote Sens. Lett.*, vol. 1, no. 4, pp. 187–194, 2010.

[27] U. Drăguţ C. Benz, P. Hofmann, G. Willhauck, I. Lingenfelder, and M. Heynen, "Multi-resolution, object-oriented fuzzy analysis of remote sensing data for GIS-ready information," *ISPRS-J. Photogramm. Remote Sens.* vol. 58, pp. 239–258, 2004.

[28] R. M. Haralick and K. Shanmugam, "Textural features for image classification," *IEEE Trans. Syst., Man, Cybern.*, vol. SMC-6, no. 6, pp. 610–621, Nov. 1973.

[29] J. W. Rouse Jr., R. H. Haas, J. A. Schell, and D. W. Deering, "Monitoring vegetation systems in the great plains with ERTS," *NASA Spec. Publ.*, vol. 351, pp. 309–317, 1974.

[30] S. K. McFeeters, "The use of the normalized difference water index (NDWI) in the delineation of open water features," *Int. J. Remote Sens.*, vol. 17, pp. 1425–1432, 1996.

[31] T. Cover and P. Hart, "Nearest neighbor pattern classification," *IEEE Trans. Inf. Theory*, vol. IT-13, no. 6, pp. 21–27, Jan. 1967.

[32] B. P. E Hart, "The condensed nearest neighbor rule," *IEEE Trans. Inf. Theory*, vol. 14, no. 14, pp. 515–516, May 1968.

[33] L. Breiman, J. Friedman, R. Olshen, and C. Stone, *Classification and Regresssion Trees*, Belmont, CA, USA: Wadsworth International Group, 1984.

[34] C. Cortes and V. Vapnik, "Support-vector networks," *Mach. Learn.*, vol. 20, pp. 273–297, 1995.

[35] R. G. Congalton and K. Green, Drăguţ. Boca Raton, FL, USA: CRC Press, 2008.

[36] C. F. Wu, J. S. Deng, K. Wang, L. G. Ma, and A. R. S. Tahmassebi, "Object-based classification approach for greenhouse mapping using Landsat-8 imagery," *Int. J. Agric. Biol. Eng.*, vol. 9, no. 1, pp. 79–88, 2016.

Filiz Bektas Balcik received the Ph.D. degree in geomatics engineering from Istanbul Technical University (ITU), Istanbul, Turkey, in 2010.

She did a part of her Ph.D. research with the International Institute for Geo-Information Science and Earth Observation, Natural Resource Department, in the Netherlands while she was a Huygens Nuffic Ph.D. Scholar (2 years). She is currently an Associate Professor with the Department of Geomatics Engineering, ITU, Istanbul, Turkey. Her research interests include remote sensing applications on land use land cover change detection, urbanization, agricultural mapping, forestry, and biophysical and biochemical characteristics of savanna vegetation, land surface temperature determination, air quality mapping using global scale remote sensing data, geographic information systems, and geostatistics.

Gizem Senel received the B.Sc. degree in 2017 and M.Sc. degree in 2019 from the Department of Geomatics Engineering, Istanbul Technical University, Istanbul, Turkey, where she is currently working toward the Ph.D. degree.

Her Ph.D. education is currently supported with scholarship by The Scientific and Technological Research Council, Turkey and Council of Higher Education, Turkey. Her research interests include remote sensing image processing, image analysis, and geographic information systems.

Cigdem Goksel received the B.Sc. degree in 1984, the M.Sc. degree in 1989, and Ph.D. degree in 1996 from Istanbul Technical University (ITU), Istanbul, Turkey.

She is currently a Professor with the Faculty of Civil Engineering, Department of Geomatics Engineering, ITU. She was a Visiting Scholar with Murray State University's Mid- America Remote Sensing Center (Geosciences), Murray, KY, USA, in 1999. Her research interests include remote sensing applications on land use land cover change detection, geographic information systems, engineering ethics, urbanization, forestry, and coastal line.